



## Optimization of sonochemical decomposition of ciprofloxacin antibiotic in US/PS/nZVI process by CCD-RSM method

Ali Reza Rahmani<sup>a</sup>, Amir Shabanloo<sup>a</sup>, Mehdi Fazlzadeh<sup>b,c</sup>, Yousef Poureshgh<sup>d,\*</sup>,  
Mohammad Vanaeitabar<sup>a</sup>

<sup>a</sup>Department of Environmental Health Engineering, School of Public Health, Hamadan University of Medical Sciences, Hamadan, Iran, Tel. +98 9181317314, email: rahmani@umsha.ac.ir (A.R. Rahmani), Tel. +98 9183786151, email: Shabanloo\_a@yahoo.com (A. Shabanloo), Tel. +98 9382099565, email: mamadtabari@yahoo.com (M. Vanaeitabar)

<sup>b</sup>Social Determinants of Health Research Center, Ardabil University of Medical Sciences, Ardabil, Iran, Tel. +98 9148090705, email: m.fazlzadeh@gmail.com (M. Fazlzadeh)

<sup>c</sup>Department of Environmental Health Engineering, School of Public Health, Tehran University of Medical Sciences, Tehran, Iran

<sup>d</sup>Department of Environmental Health Engineering, School of Public Health, Ardabil University of Medical Sciences, Ardabil, Iran, Tel. +98 9148092356, Fax +98 4533512004, email: yusef.poureshgh@gmail.com (M. Fazlzadeh)

Received 12 June 2018; Accepted 25 December 2018

### ABSTRACT

There is an increasing interest in the use of advanced oxidation process to remove antibiotic resistant compounds. The aim of this study was to optimize ciprofloxacin antibiotic decomposition in the US/PS/nZVI process using the CCD-RSM. In fixed radiation ultrasound waves with 40 KHz frequency, the influence of independent parameters such as pH of the solution, PS, and nZVI concentrations were examined in the decomposition of ciprofloxacin with a concentration of 50 mg/L in all cases. The synergy of decomposition and impact of retention time was determined after process optimization. Nanoparticles of zero valent iron were synthesized by sodium borohydride reduction. The results showed that initial pH was the most effective parameter at determined optimal values. In initial concentration of COD (195 mg/L equivalent to 50 mg/L of the antibiotic), concentration of PS and nZVI were 1200 mg/L and 120mg/L, respectively. Under these conditions, the observed removal efficiency was 57% after 60 min. For the US/PS/nZVI, synergy of decomposition was about 42.55% in optimal conditions. Almost 94% of COD was removed as a result of retention in optimal conditions after 180 min. The results of this study confirmed an acceptable performance of the US/PS/nZVI as an advanced oxidation process for ciprofloxacin decomposition.

*Keywords:* Ciprofloxacin; Ultrasound; Persulfate; Zero-valent iron nanoparticles; Optimization

### 1. Introduction

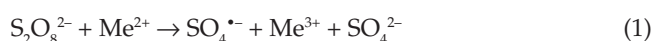
Wastewater containing antibiotic compounds such as the waste of the pharmaceutical industry is one of the environmental problems that threaten the environment [1–5]. Among the antibiotic compounds, ciprofloxacin is a well-known antibiotic in a large family of fluoroquinolones [6,7]. The presence of fluorine atoms in these antibiotics leads to drug resistance and environmental sustainability. There-

fore, the presence of these compounds in the environment is considered as a pollutant [8–10]. Antibiotic concentrations in the range of ng to mg are found in urban sewage and wastewater of antibiotic associated industries such as pharmaceutical industry, as well as livestock and poultry industries [11]. However, concentrations of these pollutants in the wastewater of pharmaceutical industry can reach 100 mg/L [12,13]. The most important environmental problems in this concentration range is antibiotic resistance of pathogens particularly microbes [14,15].

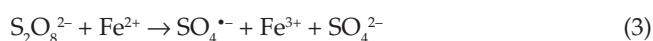
In order to remove organic and toxic compounds, the use of advanced oxidation processes has been one of the

\*Corresponding author.

options for researchers and operators of water and wastewater treatment plants in recent decades [16–21]. The persulfate anion ( $S_2O_8^{2-}$ ) or PS1 oxidation potential of 2.01 V is among the compounds used in the oxidation of organic compounds, the advantages of which include inexpensiveness, non-selective oxidation, high stability of generated radicals in different conditions, high solubility, solidness, and the easy handling and storage compared to hydrogen peroxide ( $H_2O_2$ ) [22–25]. However, studies on the application of PS in the decomposition of organic matter have shown that its decomposition kinetics at room temperature is slow, therefore, PS needs to be activated to speed up the process. Heat, ultraviolet light, and electron transfer by transition metals ( $Me^{2+}$ ) are PS activation methods. The final product of activation is sulfate radical ( $SO_4^{\bullet-}$ ) with an oxidation potential of 2.6 V [26,27]. Eq. (1) shows chemical activation of PS with transition metal [26]:



The use of divalent iron ( $Fe^{2+}$ ) as the most common transition metal has a number of disadvantages, including increased production of iron sludge and absorbance of  $SO_4^{\bullet-}$  radicals in high concentrations of iron [28–32]. Because of the problems associated with the use of this activator, nZVI or ( $Fe^0$ ) was used in this study, which can act as a permanent source of  $Fe^{2+}$  and continuously make iron in reaction with PS. The reactions of  $Fe^0$  with PS are shown in Eqs. (2) and (3) [33,34]:



Today, advanced oxidation with US waves based on acoustic cavitation is also of interest to researchers. The release of the waves in water creates micro bubbles with indoor temperature and pressure of 5000°K and 1000 atm, respectively. This condition eventually leads to the formation of  $OOH^{\bullet}$ ,  $OH^{\bullet}$ ,  $H^{\bullet}$  and  $O^{\bullet}$  radicals around the bubbles [35–37]. In this regard, Zou et al. used the heterogeneous Fenton PS/ $Fe^0$  enhanced with US for the oxidation of sulfadiazine antibiotic. In this study, the removal efficiency of antibiotics increased with increasing the ratio of PS to  $Fe^0$  from 1 to 0.1 to 1 to 1. In addition, maximum efficiency obtained at pH = 3 [38]. In the process of  $Fe^0$ /PS, Deng et al. also introduced zero-valent iron as an alternative source to activate PS instead of  $Fe^{2+}$  for acetaminophen oxidation [39].

Oncu et al. studied PS activation by heat/iron in sewage sludge treatment of antibacterial micro-pollutants using three micro-pollutants, viz. oxytetracycline, ciprofloxacin, and triclosan yielding decomposition rates of 95, 84, and 99%, respectively [40].

In the present study, to optimize the parameters of the process, central composite design and response surface methodology was used. The design of testing reduces time and costs and lead to products that have better performance of its kind and high reliability [41]. Response surface methodology is able to take into account interactions between parameters and propose a mathematical model to predict the response process [3,42,43]. In addition, finding optimal

points out of the test with an equal accuracy to experimental ones, and presenting two-dimensional and three-dimensional graphs are of other benefits of this approach [44]. A literature review indicated that there is no study related to the optimization of ciprofloxacin removal with simultaneous processing of US/PS/nZVI. Also, synergistic effects of advanced oxidation processes are not well identified. Therefore, the aim of this study was to optimize sonochemical decomposition of ciprofloxacin in US/PS/nZVI process with CCD-RSM, and ultimately to determine the synergistic effect of the components participating in the process.

## 2. Materials and methods

### 2.1. Materials

Ferrous sulfate heptahydrate, sodium borohydride, starch, ethanol, sodium hydroxide, sulfuric acid, and potassium persulfate were obtained from Merck, Germany. Ciprofloxacin HCl was purchased with a purity of 99.8% from Alborz Pharmaceutical Company (Iran). General specifications of ciprofloxacin is shown in Table 1 [45].

### 2.2. Optimization of ciprofloxacin removal

The effects of three independent parameters, including initial pH, PS concentration, and the concentration of nZVI were evaluated in process performance. The time parameter (60 min) and the concentration of antibiotics (50 mg/L) were fixed at this stage [45,46]. Quantitative range of parameters were selected based on similar studies and pre-tests and named according to Table 2, respectively. In this study, central composite design (CCD) in five levels ( $\alpha+$ , 1+, 0, 1-,  $\alpha-$ ) combined with RSM statistical methods were used to design and optimize the process using Design-Expert software Version 7.1.3. Removal efficiency was considered as the dependent variable (response). Twenty experiments were designed given the number of variables and the five levels.

### 2.3. Procedure

This experimental study was carried out in a sonochemical batch experiment reactor at the water and wastewater

Table 1  
General specifications of ciprofloxacin antibiotic (El-Shafey et al., 2012)

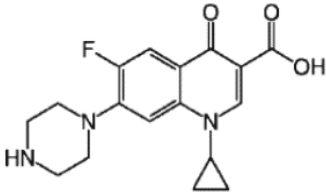
Molecular structure	
Chemical structure	$C_{17}H_{18}FN_3O_3$
Molecular weight	331.346 g·mol <sup>-1</sup>

Table 2  
Levels and range of variables to optimize ciprofloxacin removal

Variable	Sign	Unit	Levels				
			$\alpha-$	-1	0	+1	$\alpha+$
Initial pH	A	-	2.97	4.5	6.75	9	10.53
Initial concentration of PS	B	mg/L	194.33	450	825	1200	1455.67
Initial concentration of nZVI	C	mg/L	12.73	40	80	120	147.27

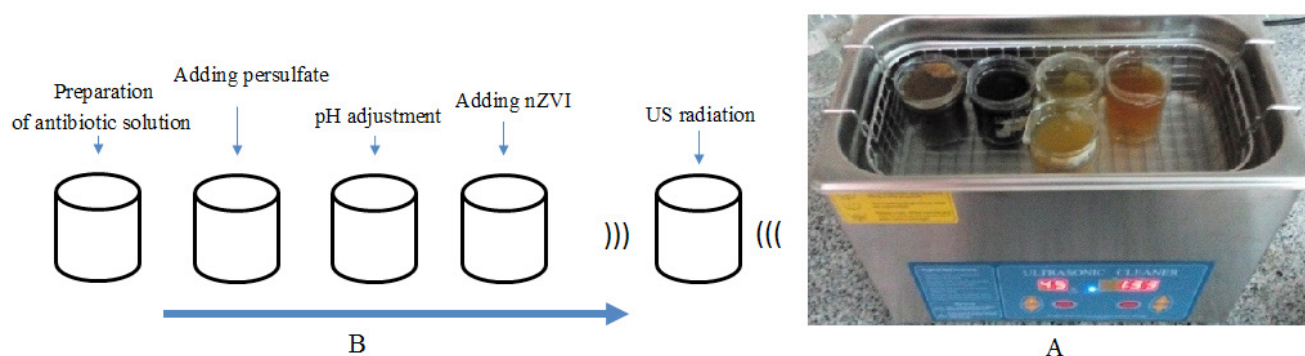


Fig. 1. (A) Overview of working reactor, (B) the preparation process of samples.

laboratory, School of Public Health, Hamadan University of Medical Sciences in winter 2014. Finally, retention times (90, 120, 180 min) and synergy of decomposition were also investigated after optimization of three key parameters. The volume of each sample was 100 mL. PS required concentration was prepared from a mother solution (1 g of potassium persulfate in 1000 mL distilled water). The pH was adjusted using sulfuric acid 0.1 M and 0.1 N. In order to prevent clotting of iron, required nZVI concentrations were added after pH adjustment. During the process (60 min), all samples were exposed to US- radiation with constant frequency (40 KHz) and power (350 W). Fig. 1 (A and B, respectively) shows the working reactors and the preparation of samples. Ciprofloxacin content in the samples was measured with COD method [47]. In order to remove the adverse effect of remaining iron on the measurement of COD, samples were aerated for 2 min, and then was centrifuged at 5000 rpm for 3 min. COD removal efficiency observed in the samples was obtained from Eq. (4) [1]. COD was measured according to 5220. C<sup>1</sup> Directive of standard book [48].

$$X = \frac{\text{COD}_0 - \text{COD}_t}{\text{COD}_0} \times 100\% \quad (4)$$

In this equation: X is COD observed removal efficiency in terms of %,  $\text{COD}_0$  is 195 mg/L, which is equivalent to 50 mg/L of ciprofloxacin,  $\text{COD}_t$  is remaining COD value at the time t, t is retention time (60 min).

#### 2.4. nZVI synthesis and determining its properties

Sodium borohydride reduction process ( $\text{NaBH}_4$ ) was used to synthesize nZVI. According to this method, about 10 g of ferrous sulfate heptahydrate ( $\text{FeSO}_4 \cdot 7\text{H}_2\text{O}$ ) was dissolved in 100 mL of 30% ethanol and 70% distilled water

mixture with a pH adjusted to 6.8. About 1.8 g of  $\text{NaBH}_4$  powder was then gradually added to the solution and mixed for 20 min. Finally, nanoparticles were separated by centrifuge at 5000 rpm, washed several times by ethanol and distilled water, and dried at ambient temperature washed for several times by ethanol and distilled water and then dried at ambient temperature [49]. The nanostructures in synthesized nZVI were verified by TEM analysis (H-800 Hitachi Japan).

### 3. Results and discussion

#### 3.1. TEM images of nZVI

TEM analysis (Fig. 2) shows the formation of a dense spherical structure with chain links in the structure of synthesized nZVI. Given the image scale, the diameter of the nanoparticles is about 12.5–50 nm. Results of TEM image analysis are in accordance with that of Yanpeng regarding the use of iron nanoparticles with microwaves for the removal of solvent blue and reactive yellow colors [50] as well as the study of Pema for absorption of antimony with nZVI [51].

#### 3.2. Test results

Table 3 shows the results of observed removal efficiency (response) in 20 samples.

#### 3.3. ANOVA results

The first step in analyzing results is selection of a suitable model for system that can predict the results with

appropriate accuracy. Thus, the quadratic model was used for this purpose. The proposed model for the system consists of three terms of single effects (A, B, C), three terms of interactive effects (AB, AC, BC), and three terms of curvature effects (A<sup>2</sup>, B<sup>2</sup>, C<sup>2</sup>). However, all of these parameters have no important effects on the model. The removal of these parameters - in terms of being significant or not significant- makes the model more convenient. ANOVA is

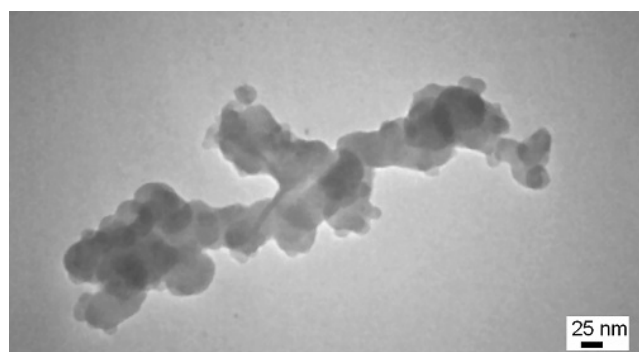


Fig. 2. TEM image of nZVI.

usually used to assess the model and to test the significance. ANOVA results (Table 4) represent the elimination of ciprofloxacin using the US/PS/nZVI. Factors with a significance level of  $p > 0.1$  for their single and interactive effects were excluded from the model. Although  $p$ -value less than 0.05 were considered significant, and those with a  $p$ -value less than 0.1 remained in the model, by which a model was developed in the system to predict the efficiency of antibiotic removal. The model includes single, interactive, and curvature factor effects. Eq. (5) shows the proposed model:

$$x' = +65.1013 - 18.193 \text{ pH} + 0.046482 \text{ PS} + 0.093629 \text{ nZVI} - 3.11 \times 10^{-3} \text{ pH} \cdot \text{PS} + 1.16313 \text{ pH}^2 \quad (5)$$

In this equation,  $X'$  COD removal efficiency (%) is the forecast, pH has no unit, PS is in mg/L, and nZVI is in mg/L.

#### 3.4. Index regression of the proposed model

Quality of the proposed model was evaluated by the coefficient of determination ( $R^2$ ) with a numeric value range of 0–1. When the  $R^2$  values are closer, model is more reliable,

Table 3

Experiments designed to remove ciprofloxacin ( $\text{COD}_0 = \text{mg L}^{-1} 195$  and time = 60 min)

No	Input variables			Response	No	Output variables			Response
	Initial pH	PS (mg/L)	nZVI (mg/L)	Removal (%)		Initial pH	PS (mg/L)	nZVI (mg/L)	Removal (%)
1	9	450	40	14.25	11	6.75	825	80	23
2	9	450	120	15.75	12	9	1200	120	32.75
3	4.5	1200	120	56.45	13	6.75	825	12.73	15.25
4	6.75	825	80	23.55	14	6.75	825	80	25.45
5	6.75	1455.67	80	35.25	15	4.5	1200	40	48.5
6	6.75	825	80	24.25	16	2.97	825	80	58/55
7	6.75	194.33	80	2.25	17	4.5	450	120	32.25
8	4.5	450	40	28.75	18	6.75	825	80	23
9	9	1200	40	24.25	19	6.75	825	80	23
10	6.75	825	147.27	30.5	20	10.53	825	80	15.5

Table 4

ANOVA results related to the ciprofloxacin removal equation

Source	Sum of squares	DF	Mean square	F-value	p-value	
Model	3770.79	5	754.16	55.91	< 0.0001	Significant
A-pH	1768.31	1	1768.31	131.09	< 0.0001	
B-PS	1247	1	1247	92.45	< 0.0001	
C-nZVI	191.56	1	191.56	14.2	0.0021	
AB	55.13	1	55.13	4.09	0.0628	
A <sup>2</sup>	508.81	1	508.81	37.72	< 0.0001	
Residual	188.85	14	13.49			
Lack of Fit	183.99	9	20.44	21.04	0.0019	Significant
Pure Error	4.86	5	0.97			
Cor. total	3959.64	19				

when  $R^2$  is greater than 0.9, the proposed model can be used to optimize the response. In this case,  $R^2$  is 0.9523 showing that the model is reasonably accurate. Review of the plot of normal function of remains:

The difference between the answer provided by the tests and fitted answer by model is called remains. The results of testing should be on a direct line to represent the normality of the data. This line is generally shown based on theoretical observation and preferably with an emphasis on the central points to the trailing. As shown in Fig. 3, they are nearly along a straight line and, thus, it can be speculated that the remains are normally distributed.

### 3.5. The effects of parameters affecting ciprofloxacin removal

Fig. 4 indicates ciprofloxacin removal efficiency as a function of pH and concentrations of PS. Fig. 5 depicts the interaction of nZVI concentration and pH effect on the removal efficiency of ciprofloxacin. Fig. 6 shows the interactive effect of PS concentration and nZVI in removal efficiency. It is observed that removal efficiency increases with increasing concentrations of PS and nZVI, and with decreasing pH values. Removal efficiency was about 57% at pH < 4.5, PS > 1200 mg/L, and nZVI concentration > 120 mg/L.

In the efficiency of chemical processes, pH is the most influential factor. In the process of PS activation by iron, pH has a direct effect on either the species or state of iron needed for PS, or to determine the dominant radical species.

At pH > 4,  $Fe^{2+}$  ions transform to  $Fe^{3+}$  that has little ability to activate PS and produce  $SO_4^{\bullet-}$  radicals. With further increases in pH,  $Fe^{3+}$  ions form ferric hydroxide increase sludge production [33]. With increasing pH, iron becomes colloidal and solid ( $Fe(OH)^+$ ), which is not able to participate in the activation process because only iron ions are able to activate PS in solution form [Eq. (6)] [52].



With further increase in pH above 9, ferric hydroxide species ( $Fe(OH)^{3+}$ ,  $Fe(OH)_4^-$ ,  $Fe(OH)_3^{\bullet}$ , and  $Fe_2(OH)_3^{4+}$ ) are produced that have little capacity for PS activation [53]. Also, changing pH activates PS with  $Fe^{2+}$  leading to the production of  $SO_4^{\bullet-}$  radicals that can somewhat drive the reaction to produce hydroxyl radical ( $OH^{\bullet}$ ), which is more likely to accrue at alkaline conditions. According to Eq. (3), a pH below 7, especially from 3 to 5, leads to production of  $SO_4^{\bullet-}$  radical. According to Eq. (7), when pH is between 7 and 9, both radicals are present in alkaline conditions of the system, particularly in a pH over 12. As shown in Eq. (8),  $SO_4^{\bullet-}$  radicals produced  $OH^{\bullet}$  in reaction with hydroxyl ions ( $OH^-$ ). Since the oxidation potential of  $OH^{\bullet}$  is highly reduced in alkaline conditions, process efficiency will be low even in prevailing presence of radicals [54].



In a study by Wang on the removal of humic acids with activated PS process by US waves, a suitable pH of 3 was

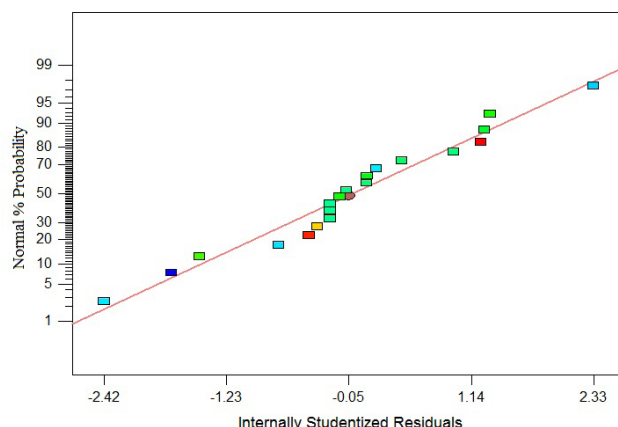


Fig. 3. Remains normal function in ciprofloxacin removal system.

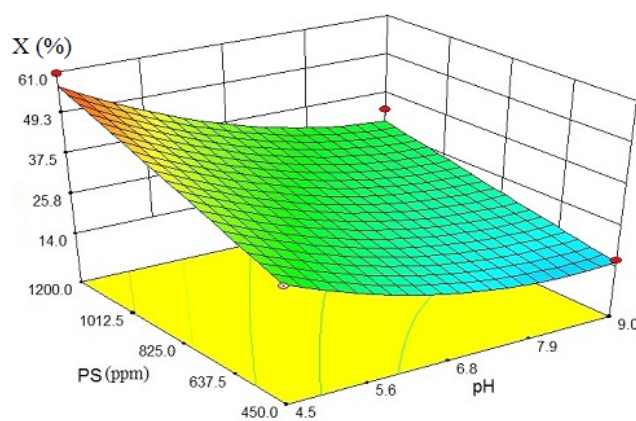


Fig. 4. Removal efficiency of ciprofloxacin as a function of pH and concentrations PS ( $COD_0 = 195$  mg/L, Time = 60 min).

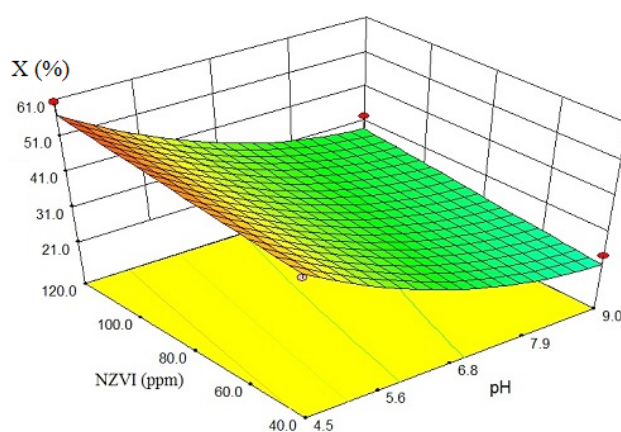


Fig. 5. Removal efficiency of ciprofloxacin as a function of pH and concentrations of nZVI ( $COD_0 = 195$  mg/L, Time = 60 min).

reported for the removal of humic acid in acidic conditions. According to Figs. 4 and 5, increasing pH in the samples decreased removal efficiency [55]. In this regard, Rao et al. examined decomposition of carbamazepine with the PS/ $Fe^{2+}$  process in an optimal pH of 3 [52]. In addition, Bagal

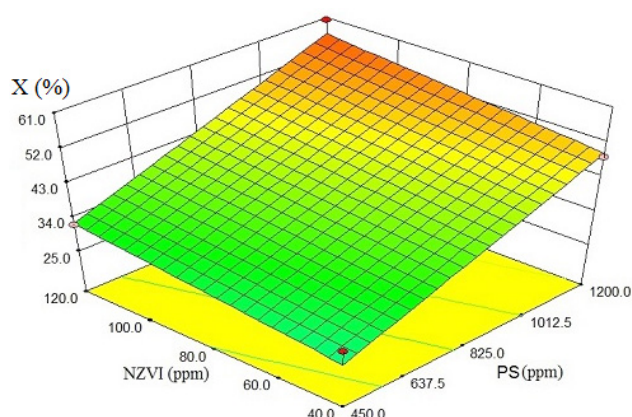
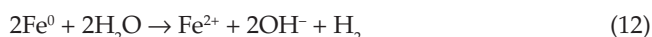


Fig. 6. Removal efficiency of ciprofloxacin as a function of PS and concentration nZVI ( $\text{COD}_0 = 195 \text{ mg/L}$ , Time = 60 min).

examined the removal of 2,4-dinitrophenol with hybrid processes based on ultrasound waves. The highest removal efficiency obtained at acidic conditions at pH of 2.5–4 [56]. In addition, in a reactor with acidic conditions, superoxide radicals ( $\text{O}_2^{\bullet-}$ ) react with hydrogen ions in the solution and produce perhydroxyl radicals ( $\text{HO}_2^{\bullet}$ ) [Eq. (9)], which finally leads to the production of  $\text{OH}^{\bullet}$  radicals [57].



In the reaction between PS and nZVI, nZVI is able to act as a resource for  $\text{Fe}^{2+}$  ions. Eqs. (10)–(13) show the production of  $\text{Fe}^{2+}$  from nZVI, among which Eq. (11) is only obtained in acidic conditions with a pH of 3. Another advantage of nZVI is that [Eq. (13)], it can reduce  $\text{Fe}^{3+}$  to  $\text{Fe}^{2+}$ , re-enter it to the cycle of activation, and reduce iron intake [39,58].



According to Figs. 5 and 6, increasing concentrations of nZVI improve ciprofloxacin removal efficiency. Optimal concentration of this parameter is 120 mg/L (Table 5). In this regard, Ghauch examined the efficiency of PS/micrometric  $\text{Fe}^0$  process for the removal of Sulfamethazole. Increasing  $\text{Fe}^0$  concentration to 2.23 mM improved the process efficiency to remove pollutants. However, the process efficiency decreased with increasing concentrations of  $\text{Fe}^0$  to 4.46, 8.92, and 8.85 mM [27]. The reasons for this decrease was the suppression phenomenon and absorption of  $\text{SO}_4^{\bullet-}$  with  $\text{Fe}^{2+}$  radicals, as in Eq. (14):



Due to limits for concentrations of nZVI, the phenomenon of efficiency reduction due to excessive increase

Table 5

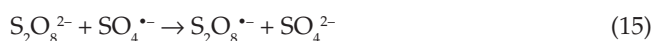
The optimal values of parameters in the removal of ciprofloxacin

System parameters	Amount
Initial pH	4.5
PS concentration, mg/L	1200
nZVI concentration, mg/L	120
Predicted removal efficiency (X'), %	57.9398
Observed removal efficiency (X), %	57

of nZVI concentration was not observed in the present study.

Increasing PS concentrations as the main source of  $\text{SO}_4^{\bullet-}$  radicals will raise efficiency. Hao investigated the amplified effect of PS on sonochemical decomposition of APFO, which had characteristics such as resistance and biological accumulation. The examined parameters were ultrasound power, concentrations of PS, pH and concentration of APFO. An efficiency of 35.5% was obtained at an initial concentration (46.4  $\mu\text{mol/L}$ ) of APFO when PS was not present for 120 min. When 10 mmol/L of the PS was added to the reaction, removal efficiency increased to 51.2%. Increasing the concentration of PS from 10 mmol/L reduced the efficiency [59]. Results presented by Hao regarding the impact of increasing concentrations of PS on increasing efficiency are consistent with the results of the present study (Figs. 4 and 6).

Regarding the concentration, increasing the concentration to a certain extent did not increase the pollutant removal efficiency, but acted as a kidnapping agent for  $\text{SO}_4^{\bullet-}$  radicals available in the aqueous solution, which reduces the process efficiency. Eq. (15) shows this phenomenon [60]:



### 3.6. Optimum conditions for the removal of ciprofloxacin and validation of models

Method of optimization in the software was used to achieve maximum removal of ciprofloxacin by determining maximization as the answer. The low limit of efficiency was set to 2.25% that was the lowest percentage observed in the experimental results. The upper limit was set to 100% because it is the highest theoretical amount. Optimum conditions predicted by the software are shown in Table 5. Optimal testing was conducted according to the parameters mentioned, and the result are presented in the same table. As can be seen, the experimental removal efficiency error is 0.94 compared to predicted efficiency. Such a little difference reflects the validity of the fit model.

### 3.7. Decomposition synergy in the US/PS/nZVI process

For this purpose, various samples of the antibiotic were prepared with an initial concentration of 50 mg/L. In each of these samples, the process lasted for 60 min, and the components participated in the process both separately and in combination with optimum conditions. Compara-

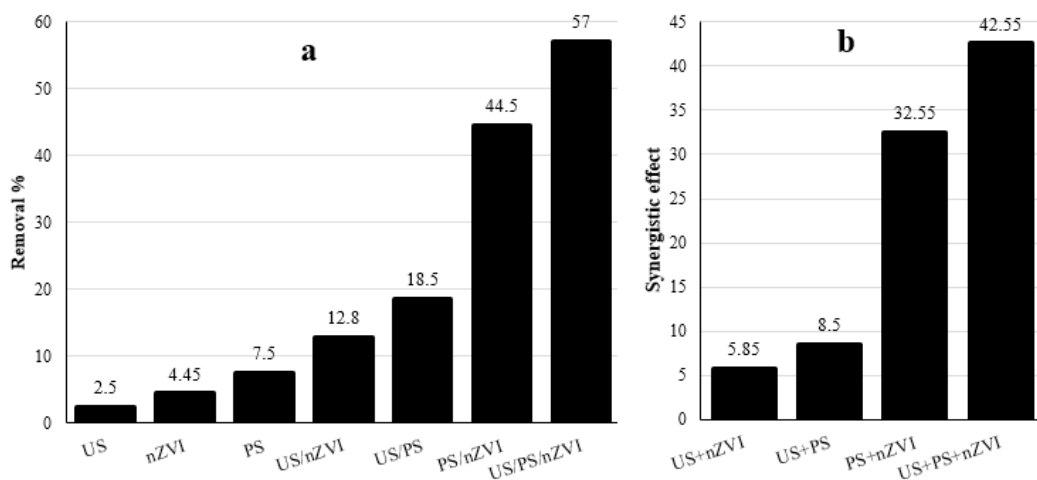


Fig. 7. (a) Removal efficiency of effective parameters in combination and separately at optimal conditions. (b) synergy of decomposition of parameters ( $\text{COD}_0$  is 195 mg/L, Time = 60 min).

tive results are shown in Fig. 7a. As specified in a separate application, PS had the highest (7.5%) removal efficiency. Combination of treatment components increased the efficiency. The synergy of decomposition in all combinative process can be seen in Fig. 7b. For example, the efficiency levels of PS and US were 7.5% and 2.5%, respectively. However, a combination of PS/US resulted in 18.5% efficiency, so the synergy in this case is calculated as: PS/US process efficiency minus (total efficiency of PS and US separately) that in this case equals 8.5%. Synergy of decomposition for US/PS/nZVI was 42.55%. The results of nZVI application are also visible in Fig. 7.

In sonochemical reactor under the direct influence of US waves on the molecules of water and oxygen,  $\text{OH}^\bullet$ ,  $\text{H}^\bullet$  and  $\text{O}^\bullet$  radicals are produced according to Eqs. (16) and (17) [61]; followed by the production of  $\text{OOH}^\bullet$  and  $\text{OH}^\bullet$  radicals [Eqs. (18) and (19)] [62].



According to Fig. 7a, the efficiency of US, nZVI, and PS in separate application to remove antibiotics were about 2.5, 4.45, and 7.5%, respectively, at optimized terms. However, when these components were put together in partnership, removal efficiency was more than the algebraic sum of separate parameters. Therefore, the synergistic effect of the process can be calculated according to Fig. 7b. In this regard, Wang et al. observed no removal efficiency in a study on the application of US/PS/ $\text{Fe}^0$  for oxidation of acid orange 7 with separate application of US, PS, and  $\text{Fe}^0$ . However, when US/PS/ $\text{Fe}^0$  were combined, about 90% of the color was removed within 20 min [63]. In a study by Liu on the application of the US/Fenton for wastewater decomposition of acid scarlet, Fenton and US separate process efficiencies were 40% and

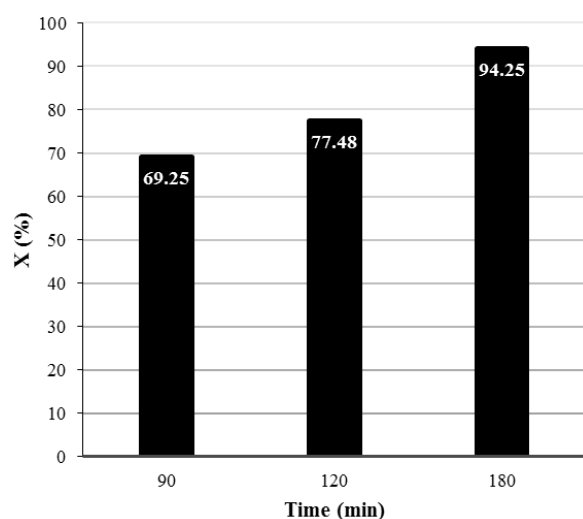


Fig. 8. The impact of retention time on COD removal under optimal conditions ( $\text{COD}_0 = 195$  mg/L).

4%, respectively. The synergy of combined US/Fenton was eye-catching with an efficiency of 90% [64]. The results of these studies are consistent with those found herein.

### 3.8. The effect of time on the removal of ciprofloxacin in optimal conditions

After optimizing pH parameters, PS concentration, and the concentration of nZVI at a fixed time of 60 min, the impact of retention time was evaluated at optimal conditions (Fig. 8). Accordingly, COD removal efficiency of antibiotics was 94.25% at the end of 180 min.

## 4. Conclusion

According to the results of this study, pH was the most important parameter influencing the process at an optimal

value of 4.5. Rising pH levels reduced removal efficiency. Optimal concentrations of PS and nZVI were 1200 and 120 mg/L, respectively. Process efficiency at optimized condition efficiency of US/PS/nZVI was 57% within 60 min. The parameters involved in the decomposition process had synergistic effects, so that the efficiency of individual processes of PS, nZVI, and US were 7.5, 4.445, and 2.5%, respectively, whereas their combined efficiency was 57%. Increasing the retention time in optimal conditions elevated removal efficiency to 94% in 180 min.

### Acknowledgment

This research has conducted by financial resources of Vice Chancellor for Research and Technology, University of Medical Sciences, Hamadan (Number: 93010235293). The authors appreciate the Deputy for their kind cooperation.

### References

- [1] M. Chen, W. Chu, Degradation of antibiotic norfloxacin in aqueous solution by visible-light-mediated C-TiO<sub>2</sub> photocatalysis, *J. Hazard. Mater.*, 219 (2012) 183–189.
- [2] M. Fazlzadeh, A. Ahmadvazeli, A. Entezari, A. Shaegi, R. Khosravi, Removal of cephalexin using green montmorillonite loaded with TiO<sub>2</sub> nanoparticles in the presence potassium permanganate from aqueous solution, 2016.
- [3] R. Shokoohi, M.T. Samadi, M. Amani, Y. Poureshgh, Optimizing laccase-mediated amoxicillin removal by the use of Box–Behnken design in an aqueous solution, *Desal. Water Treat.*, 119 (2018) 53–63.
- [4] M. Yoosefian, S. Ahmadzadeh, M. Aghasi, M. Dolatabadi, Optimization of electrocoagulation process for efficient removal of ciprofloxacin antibiotic using iron electrode; kinetic and isotherm studies of adsorption, *J. Molec. Liq.*, 225 (2017) 544–553.
- [5] S. Ahmadzadeh, A. Asadipour, M. Yoosefian, M. Dolatabadi, Improved electrocoagulation process using chitosan for efficient removal of cefazolin antibiotic from hospital wastewater through sweep flocculation and adsorption; kinetic and isotherm study, *Desal. Water Treat.*, 92 (2017) 160–171.
- [6] Y. Ji, C. Ferronato, A. Salvador, X. Yang, J.-M. Chovelon, Degradation of ciprofloxacin and sulfamethoxazole by ferrous-activated persulfate: Implications for remediation of groundwater contaminated by antibiotics, *Sci. Total Environ.*, 472 (2014) 800–808.
- [7] A.L. Capriotti, C. Cavaliere, S. Piovesana, R. Samperi, A. Laganà, Multiclass screening method based on solvent extraction and liquid chromatography–tandem mass spectrometry for the determination of antimicrobials and mycotoxins in egg, *J. Chromatography A*, 1268 (2012) 84–90.
- [8] H. Peng, B. Pan, M. Wu, Y. Liu, D. Zhang, B. Xing, Adsorption of ofloxacin and norfloxacin on carbon nanotubes: Hydrophobicity- and structure-controlled process, *J. Hazard. Mater.*, 233–234 (2012) 89–96.
- [9] M. Fazlzadeh, A. Rahmani, H.R. Nasehinia, H. Rahmani, K. Rahmani, Degradation of sulfathiazole antibiotics in aqueous solutions by using zero valent iron nanoparticles and hydrogen peroxide, *Koomesh*, 18 (2016) 350–356.
- [10] S. Ahmadzadeh, M. Dolatabadi, Electrochemical treatment of pharmaceutical wastewater through electrosynthesis of iron hydroxides for practical removal of metronidazole, *Chemosphere*, 212 (2018) 533–539.
- [11] T.M. LaPara, T.R. Burch, P.J. McNamara, D.T. Tan, M. Yan, J.J. Eichmiller, Tertiary-treated municipal wastewater is a significant point source of antibiotic resistance genes into Duluth-Superior Harbor, *Environ. Sci. Technol.*, 45 (2011) 9543–9549.
- [12] Z. Li, H. Hong, L. Liao, C.J. Ackley, L.A. Schulz, R.A. MacDonald, A.L. Mihelich, S.M. Emard, A mechanistic study of ciprofloxacin removal by kaolinite, *Colloids Surfaces B: Biointerfaces*, 88 (2011) 339–344.
- [13] A.J. Watkinson, E.J. Murby, S.D. Costanzo, Removal of antibiotics in conventional and advanced wastewater treatment: Implications for environmental discharge and wastewater recycling, *Water Res.*, 41 (2007) 4164–4176.
- [14] C. Gu, K.G. Karthikeyan, S.D. Sibley, J.A. Pedersen, Complexation of the antibiotic tetracycline with humic acid, *Chemosphere*, 66 (2007) 1494–1501.
- [15] R. Wei, F. Ge, S. Huang, M. Chen, R. Wang, Occurrence of veterinary antibiotics in animal wastewater and surface water around farms in Jiangsu Province, China, *Chemosphere*, 82 (2011) 1408–1414.
- [16] S. Parastar, S. Nasseri, S.H. Borji, M. Fazlzadeh, A.H. Mahvi, A.H. Javadi, M. Gholami, Application of Ag-doped TiO<sub>2</sub> nanoparticle prepared by photodeposition method for nitrate photocatalytic removal from aqueous solutions, *Desal. Water Treat.*, 51 (2013) 7137–7144.
- [17] R. Khosravi, M. Fazlzadehdavil, B. Barikbin, H. Hossini, Electro-decolorization of Reactive Red 198 from aqueous solutions using aluminum electrodes systems: modeling and optimization of operating parameters, *Desal. Water Treat.*, 54 (2015) 3152–3160.
- [18] A.R. Rahmani, A. Shabanloo, M. Fazlzadeh, Y. Poureshgh, H. Rezaeivahidian, Degradation of Acid Blue 113 in aqueous solutions by the electrochemical advanced oxidation in the presence of persulfate, *Desal. Water Treat.*, 59 (2017) 202–209.
- [19] A. Seid-Mohammadi, A. Shabanloo, M. Fazlzadeh, Y. Poureshgh, Degradation of acid blue 113 by US/H<sub>2</sub>O<sub>2</sub>/Fe<sup>2+</sup> and US/S<sub>2</sub>O<sub>8</sub><sup>2-</sup>/Fe<sup>2+</sup> processes from aqueous solutions, *Desal. Water Treat.*, 78 (2017) 273–280.
- [20] A.R. Rahmani, A. Shabanloo, M. Fazlzadeh, Y. Poureshgh, Investigation of operational parameters influencing in treatment of dye from water by electro-Fenton process, *Desal. Water Treat.*, 57 (2016) 24387–24394.
- [21] S. Ahmadzadeh, M. Dolatabadi, Removal of acetaminophen from hospital wastewater using electro-Fenton process, *Environ. Earth Sci.*, 77 (2018) 53.
- [22] L. Hou, H. Zhang, X. Xue, Ultrasound enhanced heterogeneous activation of peroxydisulfate by magnetite catalyst for the degradation of tetracycline in water, *Separ. Purif. Technol.*, 84 (2012) 147–152.
- [23] A. Dargahi, M. Pirsaeheb, S. Hazrati, M. Fazlzadehdavil, R. Khamutian, T. Amirian, Evaluating efficiency of H<sub>2</sub>O<sub>2</sub> on removal of organic matter from drinking water, *Desal. Water Treat.*, 54 (2015) 1589–1593.
- [24] S. Ahmadzadeh, M. Dolatabadi, In situ generation of hydroxyl radical for efficient degradation of 2, 4-dichlorophenol from aqueous solutions, *Environ. Monit. Assess.*, 190 (2018) 340.
- [25] R. Shokoohi, Y. Poureshgh, S. Parastar, S. Ahmadi, A. Shabanloo, Z. Rahmani, F.B. Asl, M.V. Tabar, Comparing the efficiency of UV/ZrO<sub>2</sub> and UV/H<sub>2</sub>O<sub>2</sub>/ZrO<sub>2</sub> photocatalytic processes in furfural removal from aqueous solution, *Appl. Water Sci.*, 8 (2018) 182.
- [26] S.-Y. Oh, S.-G. Kang, D.-W. Kim, P.C. Chiu, Degradation of 2,4-dinitrotoluene by persulfate activated with iron sulfides, *Chem. Eng. J.*, 172 (2011) 641–646.
- [27] A. Ghauch, G. Ayoub, S. Naim, Degradation of sulfamethoxazole by persulfate assisted micrometric Fe<sup>0</sup> in aqueous solution, *Chem. Eng. J.*, 228 (2013) 1168–1181.
- [28] S.-Y. Oh, S.-G. Kang, P.C. Chiu, Degradation of 2,4-dinitrotoluene by persulfate activated with zero-valent iron, *Sci. Total Environ.*, 408 (2010) 3464–3468.
- [29] M. Fazlzadeh, H. Abdoallahzadeh, R. Khosravi, B. Alizadeh, Removal of acid black 1 from aqueous solutions using Fe<sub>3</sub>O<sub>4</sub> magnetic nanoparticles, *J. Mazandaran Univ. Med. Sci.*, 26 (2016) 174–186.
- [30] M. Fazlzadeh, K. Rahmani, A. Zarei, H. Abdoallahzadeh, F. Nasiri, R. Khosravi, A novel green synthesis of zero valent iron nanoparticles (NZVI) using three plant extracts and their efficient application for removal of Cr(VI) from aqueous solutions, *Adv. Powder Technol.*, 28 (2017) 122–130.

- [31] M. Fazlzadeh, R. Khosravi, A. Zarei, Green synthesis of zinc oxide nanoparticles using *Peganum harmala* seed extract, and loaded on *Peganum harmala* seed powdered activated carbon as new adsorbent for removal of Cr(VI) from aqueous solution, *Ecol. Eng.*, 103 (2017) 180–190.
- [32] H. Abdoallahzadeh, B. Alizadeh, R. Khosravi, M. Fazlzadeh, Efficiency of EDTA modified nanoclay in removal of humic acid from aquatic solutions, *J. Mazandaran Univ. Med. Sci.*, 26 (2016) 111–125.
- [33] S. Rodriguez, L. Vasquez, D. Costa, A. Romero, A. Santos, Oxidation of Orange G by persulfate activated by Fe(II), Fe(III) and zero valent iron (ZVI), *Chemosphere*, 101 (2014) 86–92.
- [34] R. Shokouhi, Y. Poureashgh, H. Almasi, A. Shabanloo, Sonochemical oxidation of phenol using persulfate activated by zerovalent iron nanoparticles in aqueous environments, *J. Occup. Environ. Health*, 2 (2016) 7–17.
- [35] Y. Li, W.-P. Hsieh, R. Mahmudov, X. Wei, C.P. Huang, Combined ultrasound and Fenton (US-Fenton) process for the treatment of ammunition wastewater, *J. Hazard. Mater.*, 244–245 (2013) 403–411.
- [36] I. Ioan, S. Wilson, E. Lundanes, A. Neculai, Comparison of Fenton and sono-Fenton bisphenol A degradation, *J. Hazard. Mater.*, 142 (2007) 559–563.
- [37] A. Rahmani, J. Mehrilipour, N. Shabanloo, F. Zaheri, Y. Poureashragh, S.A., Performance evaluation of advanced electrochemical oxidation process with the using persulfate in degradation of acid blue 113 from aqueous solutions, *J. Sabzevar Univ. Med. Sci.*, 21 (2014) 797–807.
- [38] X. Zou, T. Zhou, J. Mao, X. Wu, Synergistic degradation of antibiotic sulfadiazine in a heterogeneous ultrasound-enhanced Fe<sup>0</sup>/persulfate Fenton-like system, *Chem. Eng. J.*, 257 (2014) 36–44.
- [39] J. Deng, Y. Shao, N. Gao, Y. Deng, C. Tan, S. Zhou, Zero-valent iron/persulfate (Fe<sup>0</sup>/PS) oxidation acetaminophen in water, *Int. J. Environ. Sci. Technol.*, 11 (2013) 881–890.
- [40] N. Bilgin Oncu, N. Mercan, I. Akmehmet Balcioglu, The impact of ferrous iron/heat-activated persulfate treatment on waste sewage sludge constituents and sorbed antimicrobial micropollutants, *Chem. Eng. J.*, 259 (2015) 972–980.
- [41] M. Roosta, M. Ghaedi, A. Daneshfar, R. Sahraei, A. Asghari, Optimization of the ultrasonic assisted removal of methylene blue by gold nanoparticles loaded on activated carbon using experimental design methodology, *Ultrason. Sonochem.*, 21 (2014) 242–252.
- [42] M. Moradi, M. Fazlzadehdavil, M. Pirsaeheb, Y. Mansouri, T. Khosravi, K. Sharafi, Response surface methodology (RSM) and its application for optimization of ammonium ions removal from aqueous solutions by pumice as a natural and low cost adsorbent, *Arch. Environ. Protect.*, 42 (2016) 33–43.
- [43] S. Ahmadzadeh, A. Asadipour, M. Pournamdari, B. Behnam, H.R. Rahimi, M. Dolatabadi, Removal of ciprofloxacin from hospital wastewater using electrocoagulation technique by aluminum electrode: Optimization and modelling through response surface methodology, *Process Safety Environ. Protect.*, 109 (2017) 538–547.
- [44] S. Ahmadzadeh, M. Dolatabadi, Modeling and kinetics study of electrochemical peroxidation process for mineralization of bisphenol A; a new paradigm for groundwater treatment, *J. Molec. Liq.*, 254 (2018) 76–82.
- [45] E.-S.I. El-Shafey, H. Al-Lawati, A.S. Al-Sumri, Ciprofloxacin adsorption from aqueous solution onto chemically prepared carbon from date palm leaflets, *J. Environ. Sci.*, 24 (2012) 1579–1586.
- [46] L.J.M. Githinji, M.K. Musey, R.O. Ankumah, Evaluation of the fate of ciprofloxacin and amoxicillin in domestic wastewater, *Water Air Soil Pollut.*, 219 (2010) 191–201.
- [47] E. De Bel, J. Dewulf, B. De Witte, H. Van Langenhove, C. Janssen, Influence of pH on the sonolysis of ciprofloxacin: biodegradability, ecotoxicity and antibiotic activity of its degradation products, *Chemosphere*, 77 (2009) 291–295.
- [48] H. Tahmasbi, M.R. Khoshayand, M. Bozorgi-Koushalshahi, M. Heidary, M. Ghazi-Khansari, M.A. Faramarzi, Biocatalytic conversion and detoxification of imipramine by the lactase-mediated system, *Int. Biodeterior. Biodegrad.*, 108 (2016) 1–8.
- [49] A. Babuponnusami, K. Muthukumar, Removal of phenol by heterogenous photo electro Fenton-like process using nano-zero valent iron, *Separ. Purif. Technol.*, 98 (2012) 130–135.
- [50] Y. Mao, Z. Xi, W. Wang, C. Ma, Q. Yue, Kinetics of Solvent Blue and Reactive Yellow removal using microwave radiation in combination with nanoscale zero-valent iron, *J. Environ. Sci.*, 30 (2015) 164–172.
- [51] P. Dorjee, D. Amarasiriwardena, B. Xing, Antimony adsorption by zero-valent iron nanoparticles (nZVI): Ion chromatography-inductively coupled plasma mass spectrometry (IC-ICP-MS) study, *Microchem. J.*, 116 (2014) 15–23.
- [52] Y.F. Rao, L. Qu, H. Yang, W. Chu, Degradation of carbamazepine by Fe(II)-activated persulfate process, *J. Hazard. Mater.*, 268 (2014) 23–32.
- [53] L. Zhou, W. Zheng, Y. Ji, J. Zhang, C. Zeng, Y. Zhang, Q. Wang, X. Yang, Ferrous-activated persulfate oxidation of arsenic(III) and diuron in aquatic system, *J. Hazard. Mater.*, 263(Part 2) (2013) 422–430.
- [54] A. Romero, A. Santos, F. Vicente, C. González, Diuron abatement using activated persulphate: Effect of pH, Fe(II) and oxidant dosage, *Chem. Eng. J.*, 162 (2010) 257–265.
- [55] S. Wang, N. Zhou, S. Wu, Q. Zhang, Z. Yang, Modeling the oxidation kinetics of sono-activated persulfate's process on the degradation of humic acid, *Ultrason. Sonochem.*, 23 (2015) 128–134.
- [56] M.V. Bagal, B.J. Lele, P.R. Gogate, Removal of 2,4-dinitrophenol using hybrid methods based on ultrasound at an operating capacity of 7 L, *Ultrason. Sonochem.*, 20 (2013) 1217–1225.
- [57] K. Ninomiya, H. Takamatsu, A. Ohnishi, K. Takahashi, N. Shimizu, Sonocatalytic-Fenton reaction for enhanced OH radical generation and its application to lignin degradation, *Ultrason. Sonochem.*, 20 (2013) 1092–1097.
- [58] M.R. Taha, A.H. Ibrahim, Characterization of nano zero-valent iron (nZVI) and its application in sono-Fenton process to remove COD in palm oil mill effluent, *J. Environ. Chem. Eng.*, 2 (2014) 1–8.
- [59] F. Hao, W. Guo, A. Wang, Y. Leng, H. Li, Intensification of sonochemical degradation of ammonium perfluorooctanoate by persulfate oxidant, *Ultrason. Sonochem.*, 21 (2014) 554–558.
- [60] C. Liang, Z.-S. Wang, C.J. Bruell, Influence of pH on persulfate oxidation of TCE at ambient temperatures, *Chemosphere*, 66 (2007) 106–113.
- [61] F. Chen, Y. Li, W. Cai, J. Zhang, Preparation and sono-Fenton performance of 4A-zeolite supported  $\alpha$ -Fe<sub>2</sub>O<sub>3</sub>, *J. Hazard. Mater.*, 177 (2010) 743–749.
- [62] V. Naddeo, V. Belgiorno, D. Kassinos, D. Mantzavinos, S. Meric, Ultrasonic degradation, mineralization and detoxification of diclofenac in water: Optimization of operating parameters, *Ultrason. Sonochem.*, 17 (2010) 179–185.
- [63] X. Wang, L. Wang, J. Li, J. Qiu, C. Cai, H. Zhang, Degradation of Acid Orange 7 by persulfate activated with zero valent iron in the presence of ultrasonic irradiation, *Separ. Purif. Technol.*, 122 (2014) 41–46.
- [64] T. Liu, F.W. He, Y.Q. Zhang, Synergistic degradation of acid scarlet dyeing wastewater by the ultrasound/fenton method, in: *Applied Mechanics and Materials*, Trans Tech Publ, 2014, pp. 34–37.